Journal Homepage: http://ijcpe.uobaghdad.edu.iq
Iraqi Journal of Chemical and Petroleum Engineering
Vol. 25 No. 2 (June 2024) 61 – 71
EISSN: 2618-0707, PISSN: 1997-4884

Pilot Area Formation Evaluation: Upper Shale Member /Rumaila Oil Field

Arafat T. Saleh [a, b, *], **Mohammed S. Al-Jawad** [b]

a Basra Oil Company, Al Basra, Iraq
b Department of Petroleum Engineering, College of Engineering, University of Baghdad, Baghdad, Iraq

Abstract

This study aims to conduct a comprehensive formation evaluation of a pilot area within the Upper Shale Member of the Rumaila Oil Field. This evaluation is an essential step in the full development of the field. The application of well-log data and core analyses can help in obtaining the desired information about the geological characteristics of the formation. The process begins with measuring the formation temperature and water resistance utilizing Schlumberger's charts and equations. The volume of shale was determined by two different methods, which were then used together to obtain the final shale volume. The porosity was determined using the conventional porosity equations from the porosity logs and the saturation was estimated based on Archie's equation. In core data analysis, an unconventional technique was utilized to determine rock type and permeability. The core porosity and the permeability were classified into four groups mainly using a self-organizing map and an unsupervised machine-learning method, and selected regression equations of each group were applied to estimate permeability in the core. The method depicted a good agreement between the core and estimated permeabilities, proving it as an effective tool. A complicated training data set was constructed based on the use of a multilayer perceptron neural network on coreless wells to identify rock types and permeability. Analyzing the petrophysical properties of the study area showed evidence that this area is characterized by heterogeneity. The heterogeneity of this formation is due to the presence of a considerable amount of shale, in addition to the significant characteristic differences in the layers and the same layer in different locations. The abundance of shale rock poses challenges during drilling operations, particularly due to shale washout which can lead to mechanical issues with the drilling string. Therefore, caution is advised when drilling new wells in the area to mitigate shale washout risks. Furthermore, the analysis identified layers with high hydrocarbon saturation that are viable for production. Conversely, some layers, characterized by shale presence and poor rock quality, are deemed unsuitable for production, and should not be considered as reservoir rock.

Keywords: Formation Evaluation; Neural network; Rock type; Permeability model.

Received on 01/06/2023, Received in Revised Form on 24/09/2023, Accepted on 27/09/2023, Published on 30/06/2024

https://doi.org/10.31699/IJCPE.2024.2.6

1- Introduction

Formation evaluation is interpreting measurements obtained within a wellbore to locate and estimate hydrocarbon reserves in the rock next to the well [1]. Formation evaluation is utilized in reservoir explorations, productions, and developments to evaluate whether a possible oil and gas resource is financially feasible. Also, it is crucial for calculating oil reserves and plays a significant part in oil economics [2]. Wireline logs are employed to characterize the reservoirs' physical features, such as saturation, porosity, and hydrocarbon movability; the shale volume is the most fundamental and foundational reservoir characteristic that describes the amount of shale that is present in hydrocarbon reservoirs. It is necessary to precisely calculate other petrophysical characteristics such as effective porosity, Net to Gross ratio, and others [3]. However, permeability is more challenging to acquire from wireline logs and will be defined in different methods [4]. Well logging gives detection, but not assessment, of a zone's permeability. Certain well logs and their findings, such as porosity logs, may be used to determine permeability by experimental correlations of log responses to core permeability data. Well logs can compute water saturation and apparent formation factor to interpret permeability from resistivity logs [5], but the porosity is utilized more often than resistivity to analyze permeability. The link between permeability and porosity may not be particularly exact because permeability is a measure of the dynamic features of the formation, while well logs only provide static readings. The study of petrophysical characteristics provides a unique opportunity to investigate the link between saturation and porosity [6]. Particularly for fragmented and poor porosity with poor sorting, the basic rule of rising permeability with rising porosity is broken. The number and size of the pore body determine porosity. Nevertheless, permeability is influenced by the amount of pore throats that traverse pore bodies or the contact per grain. As no all-inclusive method for reservoir flow zonation exists, identifying the kind of rock in

*Corresponding Author: Email: arafat.talal2108m@coeng.uobaghdad.edu.iq

hydrocarbon-bearing formations has proved difficult. Utilizing a core integration, well log, and core analysis data that considers one of the most efficient methods to reflect the reservoir's storage capacity and flow capacity with the rock type number and the complexity degree in the reservoir [7].

The most classic way to do reservoir rock type is by using a flow zone indicator (FZI). Amaefule introduced the Flow Zone Indicator concept (FZI) as the first principle to define the Hydraulic Flow Unit (HFU) based on the Carman-Kozeny model [8, 9]. However, this study used an unconventional method for classifying the reservoir rock. A cluster describes a set of data points that gather together due to particular commonalities. Cluster analysis is an unsupervised algorithm for describing a collection of observations with shared features into meaningful subgroups, i.e., the observation is sorted into a unique and uniform group called a cluster representing a type of rock. The self-organizing map, a particular kind of artificial neural network (ANN) that learns through competitive learning as opposed to error-correction learning as other ANNs do, was used to classify the groups [10]. It is a way to reduce the number of data dimensions because it is an unsupervised neural network trained using unsupervised learning techniques to build a low-dimensional, discretized representation from the input space of the training samples [11]. The rock-type process used the data of cored intervals. A correlation between the rock types and the log curves must be found to create a continuous rock type across all zones. Training the open hole basic logs for predicting rock type using a multilayer perceptron (MLP) method, MLP uses backpropagation, a supervised learning method, to train its models [12] by creating a training data set; we can predict permeabilities for the wells that have no core data. This work aims to understand the reservoir, evaluate its zones, and help make decisions about completion processes during the drilling of new wells and how to place the perforation in sections that contain oil saturation and have good rock quality. This evaluation is also an important step when building the reservoir model.

2- Reservoir Overview and Area of Study

The Upper Shale Member (USM) is a part of the Zubair formation in the Rumaila field. This member was made by a shoal water delta complex that moved northeast from the Arabian craton during the late Hauterivian to Aptian Fig. 1 [13]. The Upper Shale member forms the final back-stepping phase of the delta and is replaced distally by carbonates that climax in the overlying shallow water Shuaiba Limestone Formation [14]. This study concentrates on the pilot area, which was selected to give an overview of the whole USM. The zones of the USM are USM10, USM20, USM30, USM40 and USM50. We obtained data from one cored well and four uncorded logged wells.

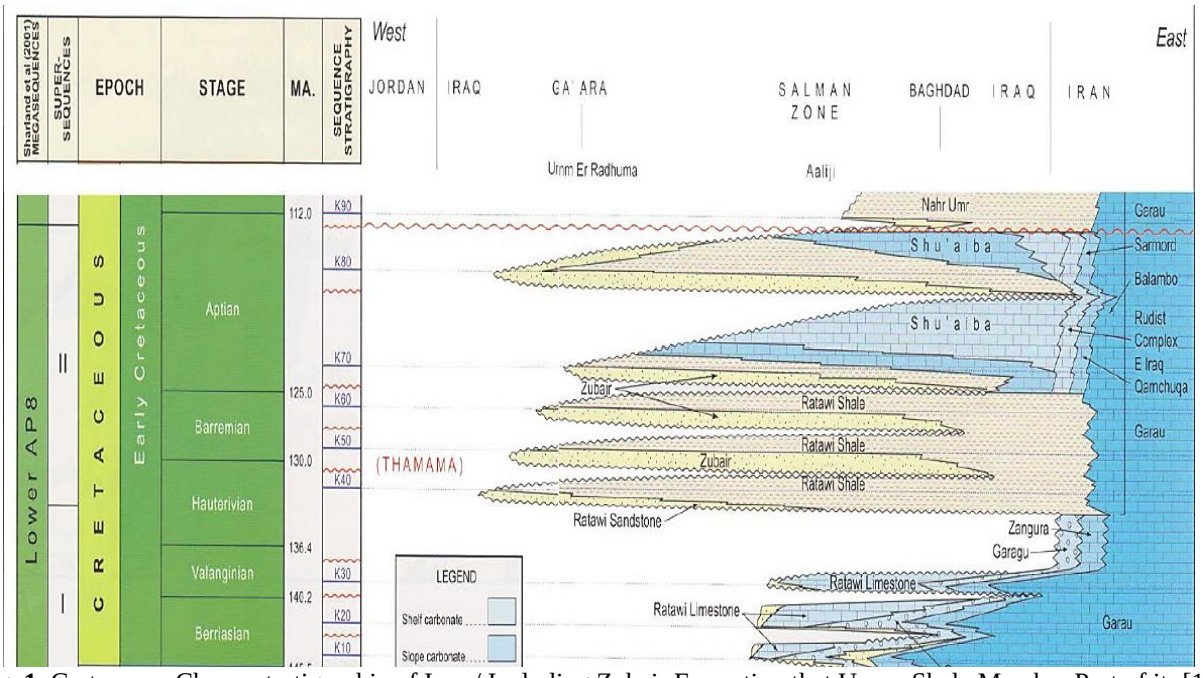

Fig. 1. Cretaceous Chronostratigraphic of Iraq / Including Zubair Formation that Upper Shale Member Part of it [13]

3- Interpretation Workflow

A qualitative and quantitative process for formation evaluation has been initiated, starting with fluid properties and ending with the permeability estimation model.

3.1. Fluid Properties

The salinity of the Zubair reservoir water aquifer is 300,000 ppm NACL [15]. The temperature measurement and water resistivity were extracted and calculated from Schlumberger charts [16] and equations, as seen in Fig. 2.

Fluid density was estimated using RHOB versus overburden-corrected core porosity cross plot, using a regression fixed at a value of 2.65, oil Leg 0.968 g/cc and water Leg 0.98 g/cc[16].

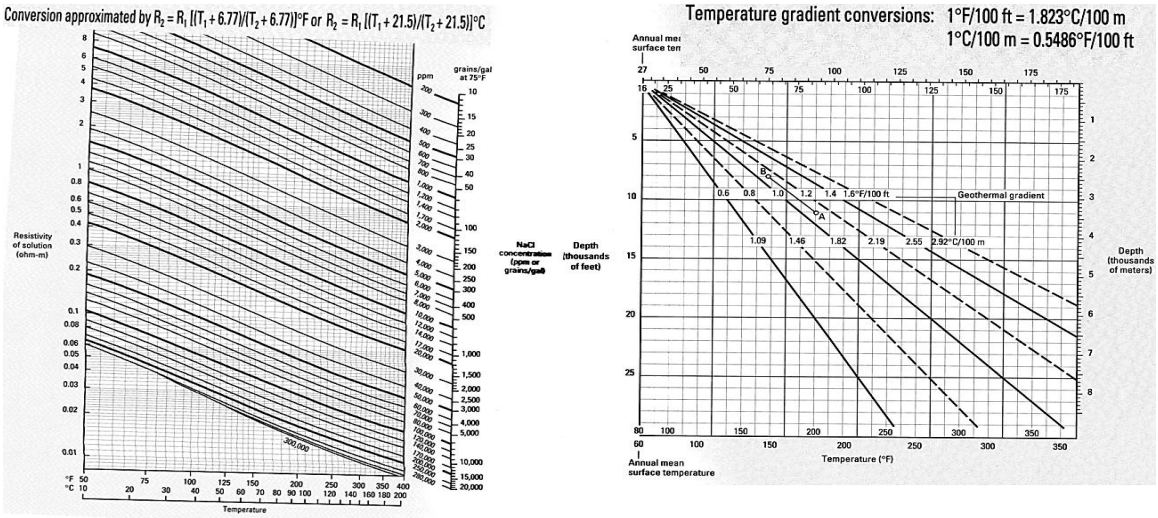

Fig. 2. The Equations for Temperature Measurement and Water Resistivity Calculation [16]

3.2. Shale Volume

Since the presence of shale lowers the reservoir's effective porosity and permeability, determining shale volume (Vshale) distribution is one of the most crucial variables that must be considered. The calculations:

A. From gamma ray

The Shale index related to shale volume, Vshale, is commonly assumed to equal the GR index [17]. The GR sand(matrix) = 18.6, and the GR shale has taken at zone USM 10, which is considered a total shale formation.

$$GR\ index = (GR - GR\ matricx)/(GR\ shale - GR\ matrix) \quad (1)$$

$$VSH = GR\ index \quad (2)$$

Where, GR: Gamma Ray reading of log. GR matrix: Gamma Ray matrix-GR log reading in 100% matrix rock (or clean sand). GR shale: Gamma-ray shale-GR log reading in 100% shale.

B. From Neutron - Density Log

Shale volume can be calculated using the density-neutron cross plot based on the density and neutron measurement in the shale rock,

Table **1** illustrates the equation parameter values input.

$$Vshale_{ND} = (\emptyset neutron - \emptyset density)/(\emptyset neutron\ shale - \emptyset density\ shale\ ). \quad (3)$$

$$Xo = NPHI\ ma \quad (4)$$

$$X1 = NPHI + M1 * (RHOP\ ma - RHOP) \quad (5)$$

$$X2 = NPHI\ sh + M1 * (RHOB\ ma - RHOB\ sh) \quad (6)$$

$$M1 = (NPHI\ fl - NPHI\ ma)/(RHOB\ fl - RHOB\ ma) \quad (7)$$

$$Vshale = (X1 - Xo)/(X2 - Xo) \quad (8)$$

Table 1. Equation Parameter Input for the Neutron Density Method

Name	Unit	Description	value
NPHI_fluid	v/v	Neutron porosity log reading in 100% water	1.0
NPHI_shale	v/v	Neutron porosity log reading in 100% shale	0.4
NPHI_matrix	v/v	Neutron porosity log reading in 100% matrix rock	-0.02
RHOB_fluid	g/cm3	Bulk density log reading in 100% water	1.0
RHOB_shale	g/cm3	Bulk density log reading in 100% shale	2.41
RHOB_matrix	g/cm3	Bulk density log reading in 100% matrix rock	2.65

The final Vshale calculated is by using merged method maximum for both Vsh method calculations (Taking the maximum values of which method gives high shale volume) as seen in Fig. 3.

3.3. Bad hole detection flag

A flag is a term to describe a place with a pore hole, a red flag for describing washout. Flags are created using the caliper to compute the bad hole flag. The caliper flag is based on the derivative of the caliper log. If the derivative is greater or less than 1, then the flag is set to 1. The derivative is calculated using the TechMath tools in Techlog software and is calculated using the following expression [18]:

$$\text{caliper} - \text{bit size} \quad (9)$$

This method was chosen over hole enlargement (caliper–bit size), as in some cases, if the washout isn't too rugose,

the density log can still read sensible values. The cutoff of -0.1 and 0.1 in were used.

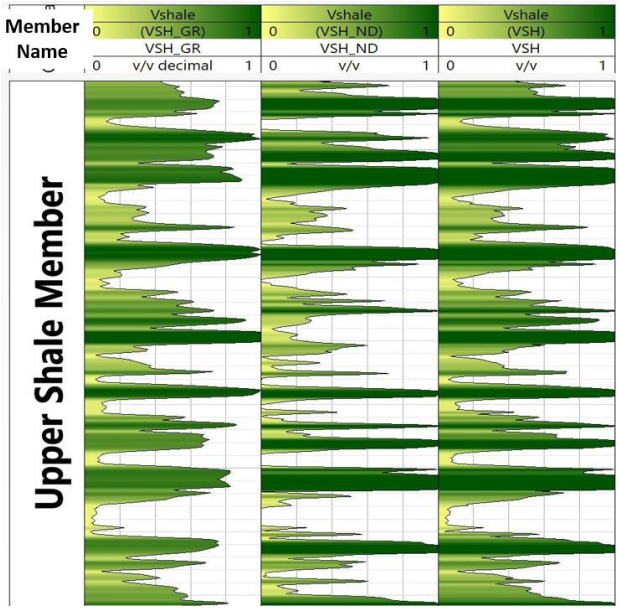

Fig. 3. Vsh Calculation Methods (Track1, Vsh from GR. Track2, Vsh from Neutron-Density). Track 3, Vsh from both Methods (Merged Method)

3.4. Porosity

Defined as a measurement of the reservoir rock's capacity to contain or store fluids [19]. The porosity is classified genetically based on the sedimentological description of the reservoir rock. The two methods that can be used to determine porosity from logs are:

A. Density Porosity (PHIT_D)

Density porosity is the preferred model where the hole condition is good and a density log is available, calculated by using the expression [17].

$$\emptyset Density = (\rho bulk - \rho matrix)/(\rho fluid - \rho matrix) \quad (10)$$

From core data, the density matrix is 2.651
Where, $\rho bulk$: Bulk Density (RHOB) log. $\rho matrix$: Matrix density of rock fabric. $\rho fluid$: Density of fluid occupying the pores in the volume investigated by the density tool.

B. Sonic Porosity (PHIT_S)

The standard Wyllie porosity was poor in the shaly sand intervals [20]. So, corrects for the shale by incorporating a variable matrix slowness in the Wyllie equation [17]:

$$PHIT_S = (\Delta t\ log - \Delta t\ Matrix)/(\Delta t\ Fluid - \Delta t\ Matrix) * \frac{1}{Cp} \quad (11)$$

$$\frac{1}{Cp} = \frac{\Delta t\ Shale(C)}{100} \quad (12)$$

Where, Δtshale = specific acoustic transit time in adjacent shales (μsec/ft,). 100 = acoustic transit time in compacted shales (μsec/ft). DT Compressional sonic (DT) log. $\Delta Matrix$ Compressional sonic travel time of the matrix ($\Delta tSand$- Sand or $\Delta tShale$ - Shale).

The matrix travel time is taken as the compressional sonic travel time for quartz from chartbooks which are 56.0 μsec/ft [19], the ΔtShale and Δt fluid are 84.1 μsec/ft,148.11 μsec/ft, respectively. The nature of the washouts in the upper shale member often causes issues for the sonic log, and sonic porosity can usually read higher than density porosity.

The final porosity PHIT curve is taken as density porosity. However, if the bad hole flag is 1 (recording washout) and the sonic porosity is less than density porosity, then sonic porosity should be used. Fig. 4 illustrates the two calculations of porosities. Fig. 4 is an example of one well data and interpretation that starts showing the zone names of the USM; the caliper shows the hole enlargement and the washout area with a grey color; the red flag indicates the washout area depending on the caliper; then, the gamma-ray log, which is used for Vshale calculation, then, the density log and the sonic log which were used for calculating the porosity. The last three columns start with the porosity from the density log, followed by the porosity from the sonic log, and the last column represents the final porosity which used in the study.

3.5. Water Saturation

Fluid saturation and porosity are the most crucial reservoir parameters for calculating oil and gas reserves. Due to the variability of most reservoirs, meaningful assessments need the continual monitoring of these parameters vs. depth. To compute the water saturation, the Archie equation is used to estimate the water saturation in sand formation reservoirs, using resistivity measurements. Archie's parameters (a, m, and n) have a more significant impact on the estimation of water saturation than resistivity. A shaly sand model is not deemed appropriate, The Archie equation is shown below [18].

$$sw^n = (a * Rw)/(\emptyset^m * Rt) \quad (13)$$

Where: a Constant, taken to be 1. m Cementation Exponent. n Saturation Exponent. ϕ Total Porosity. Rw Formation water resistivity. Rt True resistivity of the formation.

3.6. Permeability

Permeability (K) is a rock's quality measured in Darcies or milliDarcies and is determined by the size of the passageway between pores. It is calculated from core measurements directly or by empirical equations or by modeling estimation based on rock type as there is no log that can predict directly. Due to the arrangement and packing of rock grain during sedimentation [21] and as

measured across the bedding planes, the vertical permeability is lower than the horizontal permeability.

Most wells are not cored; hence the permeability of uncored portions is approximated using porosity vs. permeability calculations.

Our data contain one core well with perm/porosity measurement and four logged wells without a core. Core data used for predicting permeability modeling by using clustering methods.

The unconventional method used within this study for predicting permeability model, Principal component analysis (PCA), clustering, self-organization map (SOM), unsupervised method for classified the core date for predicting their rock type and estimating K-model.

Fig. 5. showed the distribution of the core data and how it clustered into four groups, as the author suggested. Each group is represented in a different color depending on the SOM method. For example, the red group has the highest porosity and permeability in the core data.

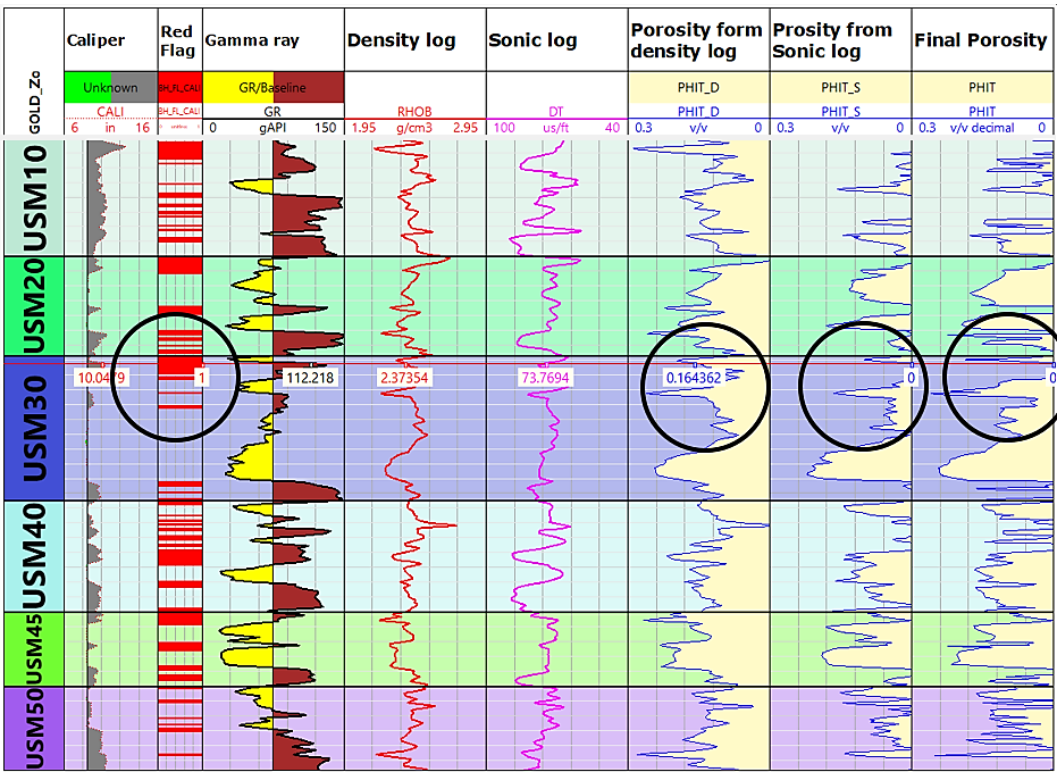

Fig. 4. Open Hole Data with Two Calculations of Porosity and the Final Porosity

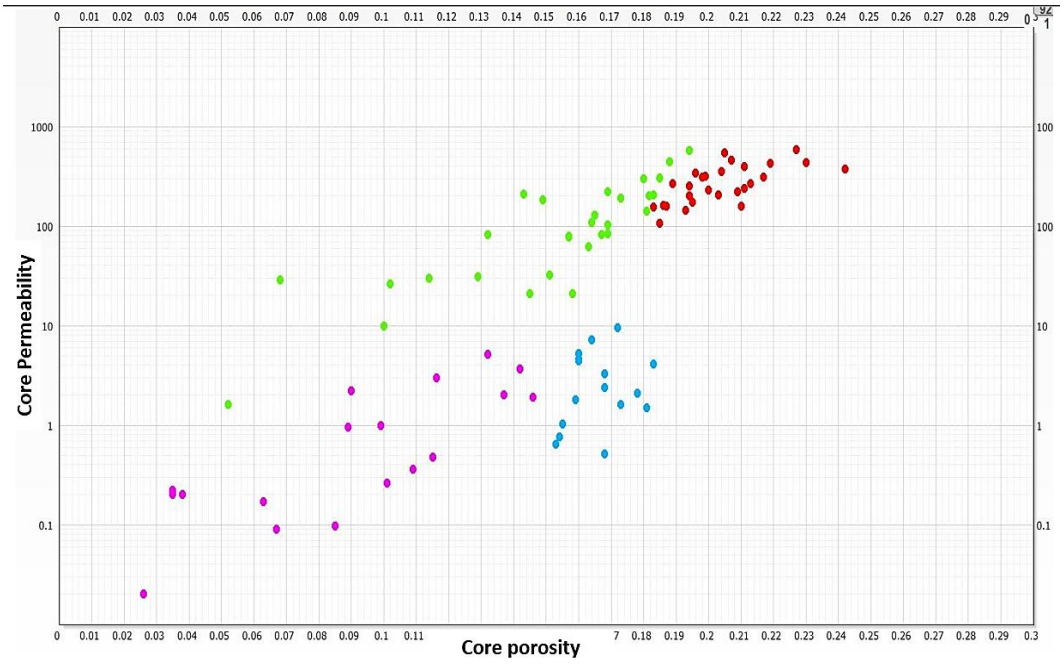

Fig. 5. Cross Plot of Core Permeability (Y axis) and Core Porosity (X axis)

For each group or cluster, an appropriate regression equation was selected for better R^2 and best fighting Fig. 6 shows the equation's best-fit function. Table 2 shows the statistics of the equations.

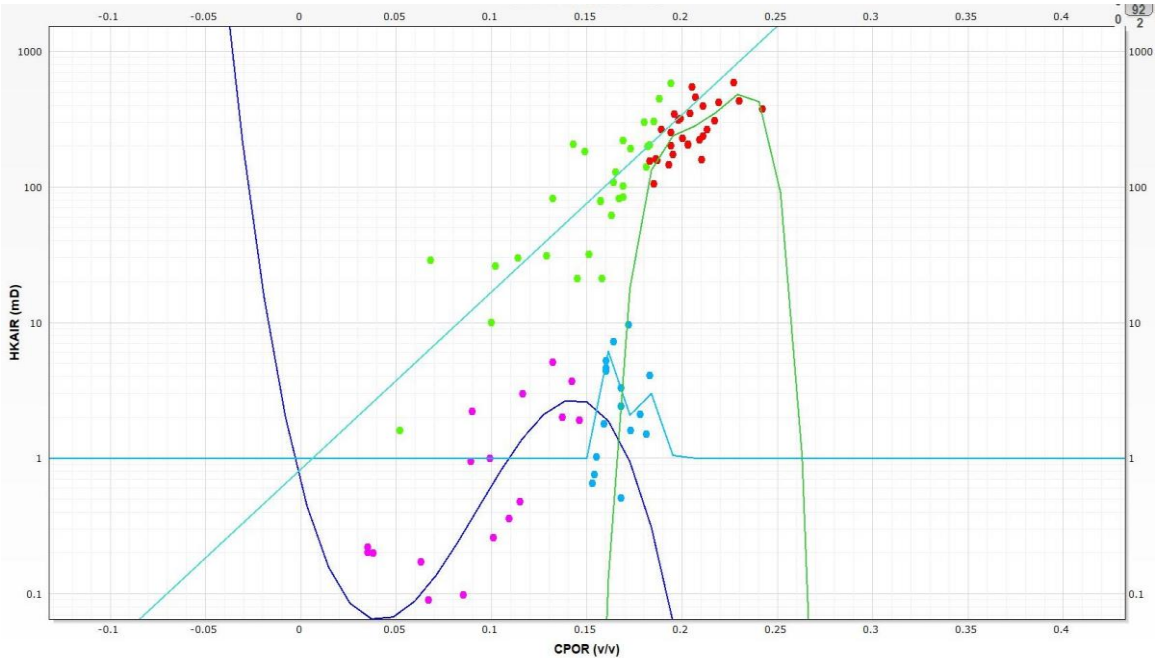

Fig. 6. Regression Best-Fit Equations for each Group

Table 2. Regression Statistics

Name	Equation	Correlation	R^2	R^2 adjusted	Number of samples	RMSE
1	log10(Perm) = 3026.7 * CPOR^3+840* Φ ^2-53.8+ Φ - 0.189	0.75	0.61	0.52	19	0.55
2	log10(log10(Perm)) = -2.5 * Φ ^4 e+7 + 1.75* Φ ^3 e+7-4614841* Φ ^2+539049.8* Φ -23575.85	0.25	0.86	0.81	13	0.24
3	log10(Perm) = 13.0767 * Φ - 0.08165605	0.83	0.70	0.72	29	0.30
4	log10(Perm) = -555639.6 * Φ ^4 + 471350.8* Φ ^3-149642.8* Φ ^2+21081.1* Φ-1109.9	0.66	0.62	0.53	28	0.14

After making the groups and expected permeability equations from the core data, there should be a way for the rest of the wells that haven't been cored to predict their permeability and rock type using the logs and the extracted classification. This was done by using a multi-layer neural network (MLP) for this purpose to train the records to predict rock type and permeability [22, 23]. The logs that were used and trained are GR, formation resistivity, compressional slowness Dt, bulk density, and neutron porosity records. Fig. 7 shows the neural network for training logs for four types of rocks.

Fig. 8 demonstrates the results that come from the clustering core data (porosity and permeability) for predicting rock type and permeability regression equations, also shows us the results of training the logs by using the MPL and their results from rock typing and estimating permeability model which compared to the core permeability. Also, Fig. 8 shows the high agreement between the core permeability, represented by red dots, and the estimated permeability, represented by a continuous dark yellow line, in the last column. Certainly, this indicates the accuracy of the rock classification shown in the columns that precede it and the accuracy of the model for calculating the permeability in this way.

By generating a training data set for the other wells with no core and depending on the core rock type results, the outcome is a permeability prediction based on their rock type for the wells with no core.

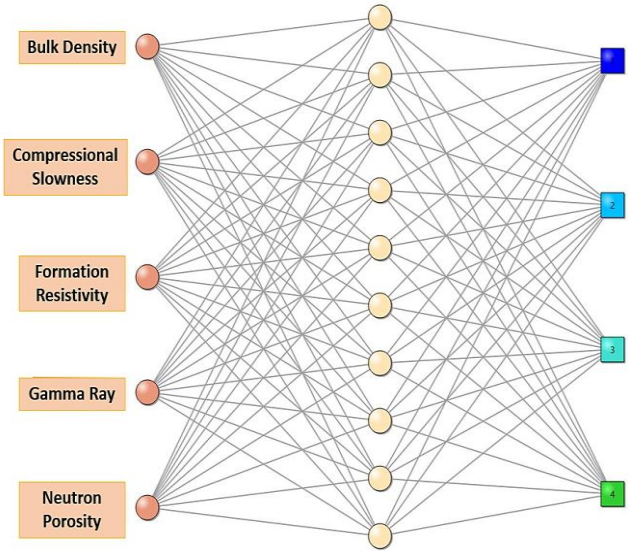

Fig. 7. Training the Logs to Predict Rock Type by MPL

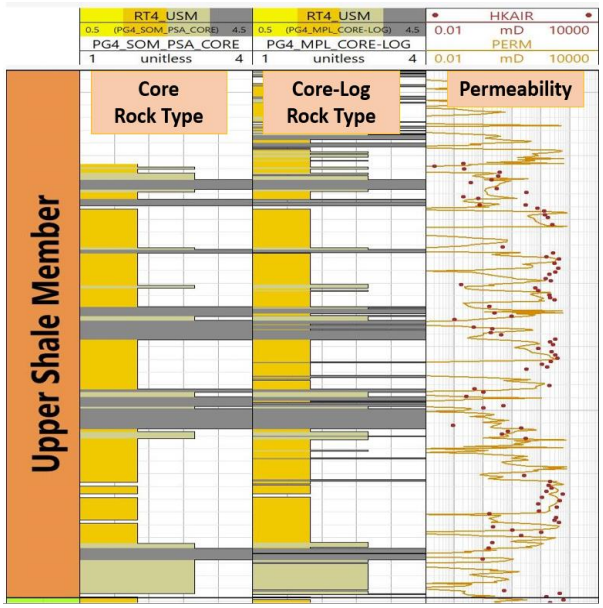

Fig. 8. Track1. Upper Shale Zone Flag, Track2. Core Rock Type, Track3. Core-Log Rock Type and Track4. The Solid Line Represents the K-Model and the Dots Represent the Core Permeability

4- Petrophysical General Overview Interpretation for the Study Area

The main goal of this study is to combine petrophysical log data so that it can be used to qualify and quantify petrophysical properties to have a quick look at the area of the study, in particular, the objectives, including determining the reservoir properties such as shale volume, porosity, fluid saturation, and permeability.

Fig. 9 shows us the general petrophysical look for the four wells, the open-hole logs, and their interpretation, which came from many equations, models, and tests on the core plugs, as well as from reservoir and geological studies of the region. Despite the distance between the wells of about 500 meters, which is a small distance, the interpretation shows the diversity of the rock properties and the diversity of fluid saturation in the zones from one well to another, also in the same zone for the same well. The sequential stratigraphic distribution of the USM within the study area, starting from USM 10 to USM 50, is shown in Fig. 9.

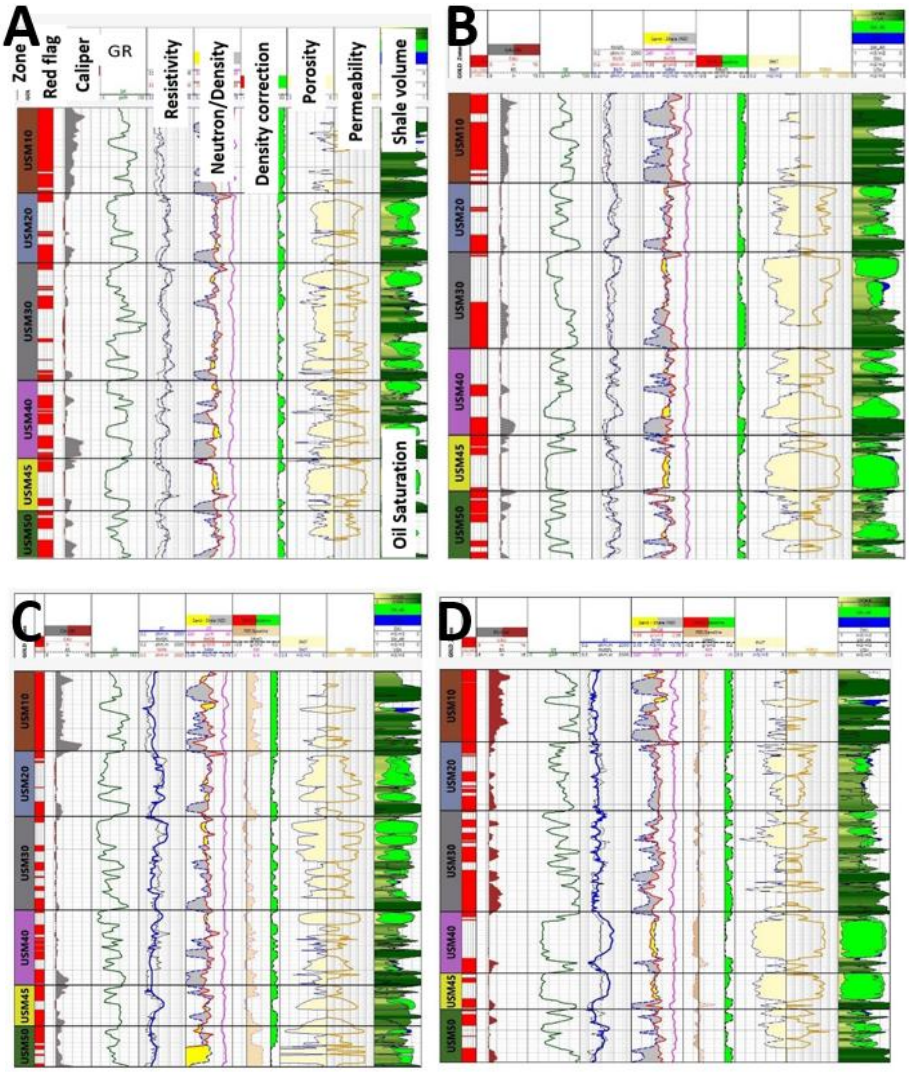

Fig. 9. Petrophysical Overview of the Studied Uncored Wells (A, B, C, and D)

For all wells, we notice the similarity of the stratigraphic behaviour of the shale or sand layers, with slight differences between one well and another. We also note that the shale separates one zone from another with a distinct thickness. We also note the calculations of porosity and permeability in all wells, which are consistent and logical with the reservoir rock. They are both high in sand rock reservoir areas that contain oil saturation. The tracks in the figure start with the name of the zone, an indication of the bad area, etc., and end with the calculations of shale volume, water saturation, and oil saturation.

The distribution of the wells that are chosen for area study is a cross-shape of five wells, with the core well in the center and four production wells in the corners. The well locations are depicted in Fig. 10. This distribution can tell us the directions of the formation and give us the best correlation depth with zones, making it clear to select the zone and also find out what changes might happen in the same direction. Although the distance between the wells is small, we can notice many changes to the nature of the pilot area or the reservoir in general, for example, the thickness of the zones, the volume of the shale rock, and the properties of the rocks (porosity, permeability, etc.).

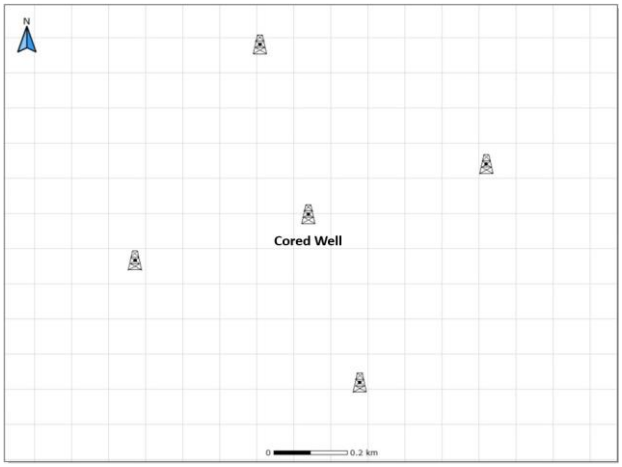

Fig. 10. Well Map Distribution

The surface orientation of the layers, as shown through the GR correlation depth from east to west, is steadily increasing; the same thing from south to north. Fig. 11 can show us the formation surface trend.

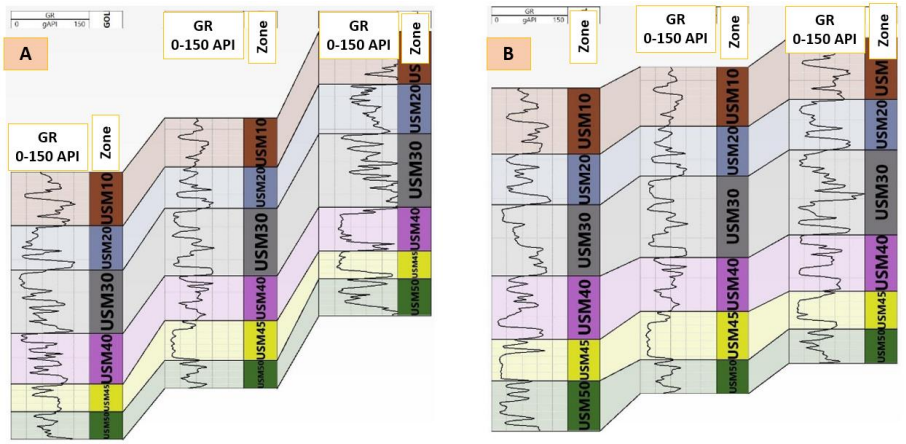

Fig. 11. A: Wells from West to East; B: Wells South to North

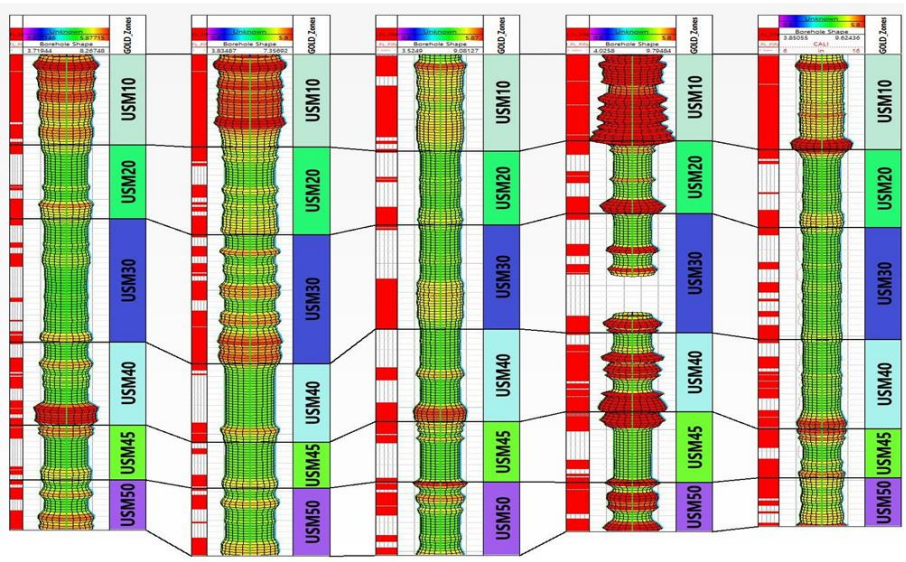

Fig. 12. Well Borehole Shape of the Five Wells Illustrating the Washout in USM

We can see the severe washout happening all the time when we have a high shale content. The washout is detected by the caliper and the density tool caliper, which were previously interpreted as bad hole flags. Fig. 12 shows the well borehole shape and the enlargement washout (the red color with the borehole drawing means out of the range of 8.5 inches, which represents the diameter of the wellbore production section). Clearly, USM10, which represents the cap rock containing a high shale proportion, was redder than the rest of the zones in the figure.

5- Conclusions

After conducting a thorough formation evaluation and in-depth analysis, the following main conclusions have been reached:

1. USM 10, the cap rock, is considered a high shale continent area; therefore, the maximum gamma ray reading (GR-shale) was used for shale volume calculation in this region.
2. The detection of bad hole conditions through caliper log provided a significant view of the hole condition and corrections.
3. The application of unconventional methods (clustering technique) yielded satisfactory results in determining rock type.
4. Permeability predictions according to the unconventional method and regression equations demonstrated a strong correlation with core data.
5. Utilizing training data set, core log correlation using neural network, and multi-layer perceptron proved to be effective in generating data sets for training logs and wells without core data.
6. Variation in zones within the Upper Shale member (USM) were observed with USM 30, USM 40 and USM45 exhibiting the highest net rock quality compared to the other zones.
7. Gamma-ray correlation indicated a stratigraphic formation direction that increases from north to south and from west to east.
8. The high shale continent of the member contributes to borehole washout during drilling activities and may cause mechanical stuck of drill pipe. Therefore, caution should be applied when drilling new wells.

Nomenclature

Hydraulic flow Unit	HFU	Shale volume	VSH
Flow zone indicator	FZI	Compressional slowness	D*T*
Artificial neural network	ANN	Total porosity	PHIT
Multilayer perceptron	MLP	Bulk density Log	RHOB
Principal component analysis	PCA	Density matrix	RHOP ma
Self-organisation map	SOM	Fluid density	RHOB fl
Gamma-ray	GR	Neutron porosity log	NPHI
Density correction	DRHO	Neutron matrix	NPHI ma
Caliper log	Calii		

References

[1] J. Quirein, S. Kimminau, J. La Vigne, J. Singer; F. Wendel, "A Coherent Framework for Developing and Applying Multiple Formation Evaluation Models," *Paper presented at the SPWLA 27th Annual Logging Symposium, Houston, Texas*, June 1986.

[2] Y. Abdul-majeed, A. Ramadhan, and A. Mahmood, "Petrophysical Properties and Well Log Interpretations of Tertiary Reservoir in Khabaz Oil Field / Northern Iraq," *Journal of Engineering*, vol. 26, no. 6, 2020, pp. 18–34. https://doi.org/10.31026/j.eng.2020.06.02

[3] V. Kamayou, C. Ehirim, and S. Ikiensikimama, "Estimating Volume of Shale in a Clastic Niger Delta Reservoir from Well Logs: A Comparative Study," *International Journal of Geosciences*, vol. 12, no. 10, 2021, pp. 949–959. https://doi.org/10.4236/ijg.2021.1210049

[4] W. Ahr, "Geology of carbonate reservoirs: the identification, description and characterization of hydrocarbon reservoirs in carbonate rocks," John Wiley & Sons, 2011.

[5] S. Saner, M. Kissami, and S. Al Nufaili, "Estimation of permeability from well logs using resistivity and saturation data," *SPE Formation Evaluation*, vol. 12, no. 1, 1997, pp. 27–31. https://doi.org/10.2118/26277-PA

[6] S. Sakurai, F. Grimaldo-Suarez, L. Aguilera-Gomez, J. Rodriguez-Larios; W. Ambrose; D. Jennette; M. Holtz; S. Dutton, T. Wawrzyniec, E. Guevara, "Petrophysical evaluation of miocene-pliocene gas reservoirs: Veracruz and Macuspana Basins, Mexico." *SPWLA Annual Logging Symposium. SPWLA*, 2002.

[7] L. Xiao, C. Zou, Z. Mao, X. Liu, X. Hu, and Y. Jin, "Tight-gas-sand permeability estimation from nuclear-magnetic-resonance (NMR) logs based on the hydraulic-flow-unit (HFU) approach," *Journal of Canadian Petroleum Technology*, vol. 52, no. 4, 2013, pp. 306–314. https://doi.org/10.2118/167255-PA

[8] J. Amaefule, M. Altunbay, D. Kersey, and D. Keelan, "Enhanced Reservoir Description: Using Core and Log Data to Identify Hydraulic (Flow) Units and Predict Permeability in Uncored Intervals/Wells," *SPE 26436*, 1993. https://doi.org/10.2118/26436-MS

[9] M. Al-Jawad., and I. Ahmed. "Permeability Estimation by Using the Modified and Conventional FZI Methods." *Journal of Engineering*, 24. 3, 2018, 59-67. https://doi.org/10.31026/j.eng.2018.03.05

[10] K. Holthausen, O. Breidbach, "Self-organized feature maps and information theory." *Network: Computation in Neural Systems*, 8.2, 1997, 215-227. https://doi.org/10.1088/0954-898X_8_2_007

[11] M. Abbas and E. Al Lawe, "Clustering analysis and flow zone indicator for electrofacies characterization in the upper shale member in Luhais oil field, southern Iraq," *Abu Dhabi International Petroleum Exhibition & Conference. OnePetro*, 2019. https://doi.org/10.2118/197906-MS

[12] M. Shateri et al., "Comparative analysis of machine learning models for nanofluids viscosity assessment," *Nanomaterials*, vol. 10, no. 9, 2020, pp. 1–22. https://doi.org/10.3390/nano10091767

[13] A. Aqrawi, J. C. Goff, A. D. Horbury and F. N. Sadooni, "The Petroleum Geology of Iraq," Scientific Press Ltd, 2010.

[14] S. N. Ehrenberg, A. A. M. Aqrawi, and P. H. Nadeau, "An overview of reservoir quality in producing Cretaceous strata of the Middle East," *Petroleum Geoscience*, vol. 14, no. 4, 2008, pp. 307–318. https://doi.org/10.1144/1354-079308-783

[15] Rumaila Operating Organization (ROO), "Rumaila Field Study Data Reference," Not Published. AL Basra, 2010.

[16] Schlumberger, "Log Interpretation Charts," 2009.

[17] Z. Bassiouni, "Theory, measurement, and interpretation of well logs," *SPE*, 1994. https://doi.org/10.2118/9781555630560

[18] Schlumberger Techlog software help center, "Techlog guru,", 2009.

[19] A. Tarek, "Working guide to reservoir rock properties and fluid flow," Gulf Professional Publishing, 2009.

[20] T. M. Müller, B. Gurevich, and M. Lebedev, "Seismic wave attenuation and dispersion resulting from wave-induced flow in porous rocks - A review," *Geophysics*, vol. 75, no. 5. Society of Exploration Geophysicists, 2010. https://doi.org/10.1190/1.3463417

[21] Y. Majeed, A. Ramadhan, A. Mahmood, "Constructing 3D Geological Model for Tertiary Reservoir in Khabaz Oil Field by using Petrel software," *Journal of Petroleum Research and Studies*, 10.2, 2020, 54-75. https://doi.org/10.52716/jprs.v10i2.350

[22] D. A. Alobaidi, "Permeability Prediction in One of Iraqi Carbonate Reservoir Using Hydraulic Flow Units and Neural Networks," I*raqi Journal of Chemical and Petroleum Engineering*, vol. 17, no. 1, 2016, pp. 1–11. https://doi.org/10.31699/IJCPE.2016.1.1

[23] O. Salman, O. F. Hasan, and S. Al-Jawad, "Permeability Prediction in One of Iraqi Carbonate Reservoir Using Statistical, Hydraulic Flow Units, and ANN Methods," *Iraqi Journal of Chemical and Petroleum Engineering*, vol. 23, no. 4, 2022, pp. 17–24. https://doi.org/10.31699/IJCPE.2022.4.3

التقييم البتروفيزياوي للمقطع التجريبي _ وحدة السجيل الاعلى لمكمن الرميلة

عرفات طلال صالح [١، ٢، *]، محمد صالح الجواد [٢]

١ شركة نفط البصرة، البصرة، العراق
٢ قسم هندسة النفط، كلية الهندسة، جامعة بغداد، بغداد، العراق

الخلاصة

تهدف هذه الدراسة إلى إجراء تقييم تكوين لمنطقة تجريبية في العضو السجيلي العلوي في حقل الرميلة النفطي، وذلك بالاعتماد على بيانات جس الابار وبيانات اللباب الصخري، وهيه من أهم الخطوات الاولية لتطوير الحقل بشكل كامل. يبدأ سير العمل بقياس درجة حرارة التكوين ومقاومة التكوين للماء؛ تم قياسها وحسابها باستخدام مخططات ومعادلات شلمبرجير. أما بالنسبة لحساب حجم الصخر السجيلي فقد تم استخدام طريقتين منفصلتين، وتم الجمع بين الطريقتين؛ ثم تم أخذ أعلى القيم التي تمثل الحجم النهائي للصخر السجيلي. أما بالنسبة للمسامية فقد تم حسابها من المعادلات التقليدية من مجسات المسامية. اما قياس التشبع، فتم استخدام معادلة آرتشي. تم استخدام تقنية غير تقليدية لتقدير انواع تصنيف الصخور والنفاذية من بيانات اللباب. تم تصنيف بيانات اللباب، المسامية و النفاذيه إلى أربع مجموعات باستخدام طريقة التعلم الآلي غير الخاضعة للرقابة، وهي خريطة ذاتية التنظيم. تم تمثيل كل مجموعة كنوع صخري، وتم اختيار معادلة انحدار تمثيلية لكل مجموعة لتقدير النفاذية. إن المطابقة المقنعة بين نفاذية اللباب ونتائج موديل النفاذية جعلت هذه الطريقة معتبرة وناجحه. بعد المطابقة، تم إنشاء مجموعة بيانات تدريبية باستخدام شبكة عصبية إدراكية متعددة الطبقات للآبار التي لا تحتوي على لباب صخري لتقدير أنواع الصخور والنفاذية لها. وبعد حساب وقياس الخصائص البتروفيزيائية لمنطقة الدراسة، أظهرت النتائج أن هذا العضو غير متجانس بسبب وجود نسب عالية من الصخر السجيلي، وكذلك بسبب الاختلاف الكبير في الخصائص من طبقة إلى أخرى وفي نفس الطبقة. يؤدي وجود نسب عالية من الصخور السجيلية إلى حدوث مشاكل ميكانيكية وهيه انحشار في سلسلة الحفر أثناء الحفر بسبب الهدم لجدار البئر؛ لذلك يجب توخي الحذر عند حفر آبار جديدة داخل المنطقة للسيطرة وتقليل الهدم للصخر السجيلي. كما كشفت النتائج أن بعض الطبقات تحتوي على نسبة عالية من التشبع الهيدروكربوني الذي يمكن إنتاجه، وبعضها بسبب وجود الصخر السجيلي وانخفاض نوعية الصخور ولا تعد صخورا مكمنية ولا يمكن الإنتاج منها.

الكلمات الدالة: تقييم الطبقات، الشبكات العصبية، انواع الصخور، موديل النفادية.